2010 IEEE International Conference on Control Applications
Part of 2010 IEEE Multi-Conference on Systems and Control
Yokohama, Japan, September 8-10, 2010

Nonlinear Model Predictive Control for the Superfluid Helium Cryogenic Circuit of the Large Hadron Collider

Rafal Noga, Toshiyuki Ohtsuka, Cesar de Prada Moraga, Enrique Blanco Viñuela and Juan Casas Cubillos

Abstract— **Superfluid helium is used in the cryogenic circuit that cools down and stabilizes temperature of more than 1600 high performance, main superconducting magnets of the Large Hadron Collider (LHC) - the new particle accelerator at European Organization for Nuclear Research (CERN). This paper presents a simulation study of the application of Nonlinear Model Predictive Control (NMPC) to the Superfluid Helium Cryogenic Circuit. First, the new first principles, distributed parameter model of the circuit to be used in online optimization is reviewed. Then stabilization of the superconducting magnets temperature using NMPC based on the model and Continuation/Generalized Minimum Residual (C/GMRES) algorithm is described. Finally the small computational cost of C/GMRES solution/approximation method and resulting real-time feasibility are highlighted.**

I. INTRODUCTION

The Large Hadron Collider (LHC) is a gigantic, 27 km circumference particle accelerator at the European Organization for Nuclear Research (CERN). The machine has established a world record in particle energy collision at 7 TeV in March 2010[1]. This achievement was possible due to the use of more than 1600 superconducting magnets, producing the very strong magnetic fields needed for guiding and focusing of particles being accelerated[2]. The high performance of the magnets has been achieved, despite their compact design, by operating them at cryogenic temperatures below 2 K, using a superfluid phase of helium 4, called He II, for cooling and thermal stabilization. The Superfluid Helium Cryogenic Circuit (SHCC), also known as the 1.8 K Cooling Loop, used for cooling down and stabilizing temperature of the LHC main superconducting magnets, was developed at CERN based on the novel concept of He II bayonet heat exchanger (BHX) [3]. The BHX is over 100 m long and is integrated into eight superconducting magnets submerged into common static bath of pressurized He II. The BHX with inner two phase flow of saturated helium at very low pressure can be regarded as quasi-isothermal heat sink and provides cooling to the magnets. The BHX and the helium bath (HB) are the main components of a 106.9 m long Standard Cell of the SHCC. More than 200 Standard Cells are present in the 27 km circumference of the LHC: 27 in each of the eight, 3.3 km long sectors.

Rafal Noga and Toshiyuki Ohtsuka are with Osaka University, 1-3 Machikaneyama, Toyonaka, Osaka 560-8531, Japan mail@rafal-noga.com

Cesar de Prada Moraga is with University of Valladolid, c/ Real de Burgos s/n., 47011 Valladolid, Spain

Enrique Blanco Viñuela and Juan Casas Cubillos are with European Organization for Nuclear Research, CERN CH-1211, Genève 23, Switzerland

The operational conditions of the cryogenic circuit are related to the thermal conductivity of He II in the HB that peaks at $T = 1.9$ K and vanishes at lambda (phase) transition temperature $T_\lambda \approx 2.17$ K. That is why the magnet's temperature should be stabilized at 1.9 K and its maximal operational value is constrained. Additional constraints are posed on maximal mass flow rate of coolant supplied to the BHX (because its overflow has to be limited, all helium must evaporate inside the BHX) and helium distribution line pumping capacity (due to the sensitivity of the cold compressors to the change in flow).

Temperature dynamics of magnets being cooled by the SHCC, Fig. 1, exhibits strong nonlinearities related to:

- heat transfers in He II being nonlinear function of local temperature gradients,
- BHX cooling power distribution, affected by BHX-HB temperature difference distribution, BHX geometry and two phase flow dynamics of saturated He II in the BHX,
- nonlinear temperature dependence of physical properties of He II: heat capacity and superfluid heat conductivity.

Significant length of the Standard Cell together with the nonlinearities result in variable dead time of response. Moreover, every two or three Standard Cells share common HB, thus are very strongly thermally coupled through heat flows in He II.

Currently the maximal temperature of LHC superconducting magnets over each Standard Cell is controlled by a separate Proportional Integral (PI) controller. The PI must be tunned in a conservative manner in order to obtain satisfactory performance at various set points and heat loads magnitudes. In order to assure that no helium overflows the BHX, the set point for the PI must be kept well above the BHX temperature, to keep high evaporation rate, thus must be adjusted in presence of the BHX temperature perturbations. The simulated PI performance is presented in Fig. 2. Please note that the closed loop dynamics changes as heat loads over two cells increase and that the thermal coupling between two neighbor cells is so strong, that both are cooled by one BHX - coolant mass flow rate into the other BHX is almost zero.

Nonlinear Model Predictive Control (NMPC), if applied to the circuit, could take into account the nonlinear system dynamics, couplings between cells, respect constraints related to maximal magnet temperature and allow operating closer to constraints posed by heat exchanger overflow. That would result in better stabilization performance at lower temperatures, thus increasing the safety margin for circuit operation.

978-1-4244-5363-4/10/$26.00 ©2010 IEEE

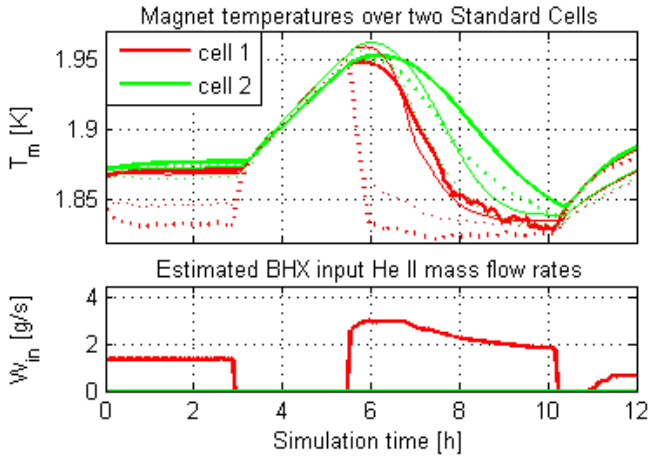

Fig. 1. SHCC dynamics: simulated using simplified model (bold lines) vs. experimental (thin lines). In the upper plot, four magnet temperatures correspond to maximal (solid line) and minimal (dotted line) value in each of two interconnected Standard Cells.

Linear and nonlinear model based controllers developed for versions of the SHCC used in LHC prototypes, String1 and String2, and Inner Triplets had good performance [4], [5], [6], [7]. Application of NMPC for 106.9 m long version of the SHCC, used for cooling of main LHC superconducting magnets, is currently under study. The goal is to develop a new, first principles, distributed parameter model of the magnet temperature dynamics and to use it to implement NMPC for stabilization of the temperature.

This paper presents preliminary results from the study. This section introduced the SHCC and the motivation for the NMPC development. Next, the first principles model of the circuit, to be used in online optimization, is reviewed and interesting features of the circuit dynamics are highlighted. Stabilization of the superconducting magnets temperature performed using NMPC based on the model and Continuation/Generalized Minimum Residual (C/GMRES) algorithm is then described and simulation results discussed. Finally, the very small computational cost of C/GMRES solution/approximation method and resulting real-time feasibility are highlighted.

II. FIRST PRINCIPLES MODEL OF THE SHCC

In the previous, first principles, simplified model of SHCC versions used in Inner Triplet and LHC Prototypes, the distribution of magnet temperatures over length of the circuit has been neglected but the dynamics of He II mass distribution in the BHX has been modeled. This approach performed well for shorter versions of the cryogenic circuit, see [4], [5], [6].

The Standard Cell of the SHCC used for cooling the main LHC magnets is a longer version of the cryogenic circuit and is thermally coupled to its neighbor cells. That is why, in contrast to previous model, the new simplified model describes the temperature distribution over the circuit length and resulting heat flows in the He II, also some to neighbor cells. This allows simulation and optimization of interconnected Standard Cells operation, up to whole sector of the LHC. But the dynamics of superfluid mass distribution in the BHX have been neglected in the new model.

The simplified model is targeted for use in online optimization of the feedback control action in frame of NMPC. In order to enable fast optimization, the model captures only most important features of the nonlinear process dynamics and uses approximations with continuous and smooth functions where needed, thus allowing explicit evaluation of Jacobians of the Hamiltonians used in optimization. Moreover, the model provides raw prediction of BHX overflow, thus allowing the NMPC to respect this operational constraint.

First principles approach to modeling allows good modeling of non-linearities of the temperature dynamics that originate at known circuit geometry and physical properties of He II. He II phase transition occurs at T_λ that constrains the model validity. However, due to approximations used, the model validity is further limited to typical SHCC operational magnet temperature range: $1.85\,\mathrm{K} < T_m < 2\,\mathrm{K}$. The controlled input variable in the circuit is the valve position, regulating liquid helium mass flow rate into the BHX. However, the relation between the two quantities contains terms coupled with the magnet temperatures, thus the mass flow is directly used as model input.

Some of the modeling errors appear due to simplifications and approximations of description of physical processes governing the circuit dynamics. For example, due to neglecting the dynamics of He II in the BHX, at specific operational conditions corresponding to low HB-BHX temperature differences, helium accumulates in the BHX and if rapid changes of cooling power occurs at this condition, a significant error in model dynamics will be observed. Errors are also introduced during spatial discretization of the Distributed Parameter System. Model validation for a full range of operational scenarios has yet not been performed. However preliminary results are very promising, see Fig. 1.

In the following subsections some key elements of the model are reviewed.

A. Dynamics of superconducting magnets temperature

The simplified model enables calculation of the dynamics of 1D distributed value of superconducting magnet temperatures in a Standard Cell of the SHCC. The dynamics is assumed to be equivalent to HB temperature dynamics and is described based on energy conservation in the HB, using $q = \frac{\partial Q}{\partial t}$, L and M for for heat transfer rates, HB length and mass respectively:

$$\frac{\partial T_m(x,t)}{\partial t} = c_v^{-1}\left(T_m\right)\frac{L}{M}\left(\frac{\partial q_{hl}}{\partial x} - \frac{\partial q_{cool}}{\partial x} - \frac{\partial q_{He}}{\partial x}\right), \tag{1}$$

for $0 < x < L$ and Neumann boundary conditions expressed using function $f\left(q\right)$ corresponding to properties of interconnection between Standard Cells

$$\frac{\partial T_m(0,t)}{\partial x} = f\left(q\left(0,t\right)\right), \quad \frac{\partial T_m(L,t)}{\partial x} = f\left(q\left(L,t\right)\right). \tag{2}$$

The linear density of sum of heat loads into the bath $\frac{\partial q_{hl}}{\partial x}$ is assumed to be constant over HB length, however its value

changes over time and represents an important perturbation to the system. The inverse of He II specific heat capacity $c_v^{-1}(T_m)$ can be approximated in the temperature range $1.85\ \mathrm{K} < T_m < 2\ \mathrm{K}$ using first order polynomial. The PDE (1) is discretized using finite volume approach.

B. Heat transfer in the superfluid helium

Heat transfer in He II is very effective at moderate heat fluxes, however it introduces strong nonlinearities and stiffness into the circuit dynamics [8]. In 1D, heat flux in He II $\frac{q_{He}}{A_m}$ is approximated using pseudo conduction therm called Superfluid Thermal Conductivity Function $F(T,p)$:

$$\left(\frac{q_{He}}{A_m}\right)^3 = -F(T_m,p)\frac{dT_m}{dx}. \tag{3}$$

Magnets operational temperature corresponds to the maximum of super fluid conductivity $F(T,p)$ that is approximated with constant value $F^{\frac{1}{3}} = 2.5\times10^4$. The resulting gradient of internal heat flow in HB

$$\frac{\partial q_{He}}{\partial x} = -\frac{A_m}{3}F^{\frac{1}{3}}\left|\frac{\partial T_m}{\partial x}\right|^{-\frac{2}{3}}\frac{\partial^2 T_m}{\partial x^2} = -k\frac{\partial^2 T_m}{\partial x^2}. \tag{4}$$

Please notice that k, corresponding to value of local thermal conductivity, is very high at small temperature gradients

$$k = \frac{A_m}{3}F^{\frac{1}{3}}\left|\frac{\partial T_m}{\partial x}\right|^{-\frac{2}{3}}, \quad \lim_{\frac{\partial T_m}{\partial x}\to 0} k = \infty, \tag{5}$$

resulting in very fast local temperature dynamics. Thus the ODE set obtained after spatial discretization of PDE (1) will be stiff if $\frac{dT_m}{dx}_i$ approaches zero at any of discretization points i. The stiffness is reduced in the simplified model using following approximation

$$q_{He} \approx -A_m F^{\frac{1}{3}}\frac{\partial T_m}{\partial x}\left(\left(2\Delta_{\frac{dT_m}{dx}}\right)^2 + \left(\frac{\partial T_m}{\partial x}\right)^2\right)^{-\frac{1}{3}}. \tag{6}$$

The approximation introduces temperature gradient errors bounded by $\Delta_{\frac{dT_m}{dx}}$, whose value has been chosen to be equal to the measurement uncertainty. Resulting maximal value of thermal conductivity k_a has been significantly reduced:

$$\lim_{\frac{\partial T_m}{\partial x}\to 0} k_a = AF^{\frac{1}{3}}c^{-\frac{1}{3}}. \tag{7}$$

C. Cooling power of the BHX

Cooling power of the BHX is identical to heat flow rate due to conduction from the HB into the BHX. It is limited by thermal resistance of the BHX that, at cryogenic temperatures, is dominated by Kapitza resistance. Resulting cooling power distribution over the BHX is expressed in terms of the Kapitza coefficient C_K, temperature difference between HB (magnets) and BHX $T_m - T_{bhx}$, T_{bhx} and inner perimeter of the bayonet heat exchanger tube wetted by He II P. Assuming that BHX temperature is equal to saturation temperature of He II $T_{bhx} = T_s$:

$$\frac{\partial q_{cool}}{\partial x} = \begin{cases} (T_m - T_s)\, C_K P T_s^3 & \text{if } T_m > T_s \\ 0 & \text{otherwise.} \end{cases} \tag{8}$$

The value of Kapitza coefficient can be experimentally estimated as being $C_K = 1200\ \mathrm{W}\cdot\mathrm{K}^{-4}\cdot\mathrm{m}^{-2}$[9]. T_s is function of very low pressure in the BHX, thus changes of pressure represent important perturbation to the circuit. In case of two phase, stratified flow, the BHX wetted perimeter P is related through the BHX geometry to the fraction of BHX cross section area occupied by saturated He II A_{SF} as $P \approx 0.839 A_{SF}^{\frac{1}{3}}$, that is related to He II mass flow rate W through He II density $\rho = 145\ \mathrm{kg}\cdot\mathrm{m}^{-3}$ and the average velocity of the He II flow v as $A_{SF} = \frac{W}{\rho v}$.

The He II flow dynamics in the BHX has been neglected in order to obtain computationally inexpensive approximation of the He II mass distribution in the BHX and based on the observation that in wide range of operational conditions, the distribution is determined by slowly changing He II evaporation rate. Thus the wetted BHX perimeter is related to mass flow using v as constant parameter

$$P = 0.16\left(\frac{W}{v}\right)^{\frac{1}{3}}. \tag{9}$$

Mass conservation principle for the steady flow connects the He II mass flow rate distribution and evaporation rate density $\frac{\partial W_{l2v}}{\partial x}$

$$\frac{\partial W}{\partial x} = -\frac{\partial W_{l2v}}{\partial x} = -\Delta_H^{-1}\frac{\partial q_{cool}}{\partial x}, \quad W(0) = W_{in} \tag{10}$$

with the latent heat of evaporation of He II $\Delta_H = 23.4\times10^3$ J/kg. Please notice the strong nonlinearities in the cooling power distribution, since it is available only for positive temperature difference $T_m - T_s$ and nonnegative mass flow W.

III. NMPC USING C/GMRES METHOD

In this section preliminary results from application of NMPC for the SHCC are presented. First, the NMPC setup using C/GMRES algorithm is described. Then simulation results are discussed and finally the observed very low computing cost and resulting real time feasibility of the C/GMRES algorithm are highlighted.

The notation used in this section has changed to the standard one used in control engineering, in contrast to physics notation used in the previous section to describe the model. Let $x(t) \in \mathbb{R}^n$ be the state vector, and $u(t) \in \mathbb{R}^{m_u}$ be the input vector of a general nonlinear system. In case of the cryogenic circuit, these correspond to discretized HB temperature T_m and input helium mass flow rate W_in respectively.

In NMPC, also known as Receding Horizon Control (RHC), optimal control problem is solved at each time t over finite time horizon. At time t, only initial value of the optimal input trajectory, corresponding to the current time t, is used as the current input to the system, which results in a state feedback control law. The optimal control problem is solved over the horizon taken from the current time t to T ahead:

$$\text{minimize } J = \phi(x(t+T)) + \int_t^{t+T} L(x(t'),u(t'))\,\mathrm{d}t', \tag{11}$$

subject to equality constraints corresponding to system dynamics

$$\dot{x} = f(x(t), u(t)) \tag{12}$$

and an arbitrary m_c dimensional vector-valued function

$$C(x(t), u(t)) = 0. \tag{13}$$

Current state $x(t)$ is used as the initial state. The problem can be reformulated using Lagrange multipliers $\lambda(t)$ and $\mu(t)$ as

$$\text{minimize } \bar{J} = \phi + \int_t^{t+T} \left[L + \lambda^T (f - \dot{x}) + \mu^T C \right] \mathrm{d}t'. \tag{14}$$

The necessary condition for an extremum of $\bar{J}$, found based on calculus of variation, can be expressed using Hamiltonian $H = L + \lambda^T f + \mu^T C$ as equations (12) and (13) enhanced by the costate differential equation

$$\dot{\lambda} = -H_x^T(x, u, \lambda, \mu), \quad \lambda(t+T) = \phi_x^T(t+T) \tag{15}$$

and the variation

$$\delta\bar{J} = \int_t^{t+T} \left[H_u(x, u, \lambda, \mu)\delta u(t') + C^T(x, u)\delta\mu(t') \right] \mathrm{d}t' \tag{16}$$

must be zero for arbitrary $\delta u(t)$ and $\delta\mu(t)$ [10]. Based on the observation that $x(t)$ and $\lambda(t)$ can be integrated for given $u(t)$ using differential Equations (12) and (15), the remaining unknowns are functions $u(t)$ and $\mu(t)$.

To solve the optimal control problem numerically, we divide the control horizon into N intervals of length $\Delta t = \frac{T}{N}$ and parametrize $u(t)$ and $\mu(t)$ using N discrete values of $u_i^*(t)$, $\mu_i^*(t)$

$$u(t) = \sum_{i=0}^{N-1} \sigma_i(t) u_i^*(t) \quad \mu(t) = \sum_{i=0}^{N-1} \sigma_i(t) \mu_i^*(t) \tag{17}$$

and N basis window functions:

$$\sigma_i(t) = \begin{cases} 1 & \text{if } t + i\Delta t \le t' < t + (i+1)\Delta t \\ 0 & \text{otherwise.} \end{cases} \tag{18}$$

Now the variation

$$\delta\bar{J} = \sum_{i=0}^{N-1} \int_{t+i\Delta t}^{t+(i+1)\Delta t} \left[H_u \mathrm{d}u_i^*(t) + C^T \mathrm{d}\mu_i^*(t) \right] \mathrm{d}t'$$

must be zero for arbitrary differentials $\mathrm{d}u_i^*$ and $\mathrm{d}\mu_i^*$. Thus the necessary condition of optimality are

$$\int_{t+i\Delta t}^{t+(i+1)\Delta t} H_u \mathrm{d}t' = H_{u,i} = 0 \quad \text{for } i = 0 \dots N-1 \tag{19}$$

$$\int_{t+i\Delta t}^{t+(i+1)\Delta t} C \mathrm{d}t' = C_i = 0 \quad \text{for } i = 0 \dots N-1. \tag{20}$$

These can be assembled into a $(m_u + m_c)N$ dimensional nonlinear equation,

$$F(U(t), x(t), t) := [H_{u,0}\ C_0^T\ \cdots\ H_{u,N-1}\ C_{N-1}^T]^T, \tag{21}$$

using

$$U(t) := [u_0^{*T}(t)\ \mu_0^{*T}(t)\ \cdots\ u_{N-1}^{*T}(t)\ \mu_{N-1}^{*T}(t)]^T. \tag{22}$$

Note that for a given sequence of discrete future inputs $\{u_i^*\}_{i=0}^{N-1}$ and Lagrange multipliers $\{\mu_i^*\}_{i=0}^{N-1}$, the state trajectory $x(t')$ over the finite horizon $t < t' < t+T$ is found by integration of the ODE corresponding to system dynamics, starting from $x(t)$. Then the costate trajectory $\lambda(t')$ is found by integration of $\dot{\lambda}$ backwards from $t+T$ back to t. Any numerical method can be used to integrate the ODE's. Finally $H_u(t')$ and $C(t')$ are evaluated and the integrals $H_{u,i}$ and C_i are calculated numerically, giving the residuum of the necessary condition of optimality F.

A. C/GMRES method

In the NMPC, at each time t, the nonlinear equation $F(U(t), x(t), t) = 0$ needs to be solved with respect to $U(t)$ for the measured state $x(t)$. Solving $F(U) = 0$ using such an iterative algorithm as the Newton method is computationally demanding. However, since F is solved continuously, its solution - the optimal input trajectory U(t) - is expected to change slowly over time as the state of the controlled system evolves and the control horizon moves. Based on this observation, in order to reduce the computational cost we employ the C/GMRES algorithm to trace the time-varying solution without any iterative searches. For comprehensive description of C/GMRES, we refer the reader to [11].

B. Optimal control problem setup

The performance of the NMPC for a given system is determined by the control objectives, expressed using cost function $L(x(t), u(t))$, and constraints defined using function $C(x(t), u(t))$. In the preliminary study, no perturbation of the BHX pressure (saturation temperature) are considered. In this case, the BHX temperature is always low enough to ensure high coolant evaporation rate at optimal magnets temperature, the setpoint $x_{sp} = 1.9$ K, thus constraints related to heat exchanger overflow and magnet maximal temperature are unlikely to be violated. That is why the constraint set is reduced to one inequality constraint on input mass flow rate $0 < u(t) < u_{max} = 10$ g/s, related to control valve capacity. This inequality constraint is expressed as equality constraint, using dummy input variable u_d:

$$(2u - u_{max})^2 + u_d^2 - u_{max}^2 = 0. \tag{23}$$

The goal of the control action is to stabilize the maximum state (temperature) value at prescribed level $\max x(t) = x_{sp}$. In order to approximate this objective a scalar asymmetric quadratic cost function is evaluated for every component $(x)_i$ of state vector x in form:

$$f_{qa}((x)_i, r, a) = \frac{[((x)_i^2 + r^2)^{\frac{1}{2}} + a(x)_i]^2 - 2ar(x)_i - r^2}{(1+a)^2} \tag{24}$$

with parameters r and a to be tuned. In order to obtain well posed optimization problem, additional weights are used: quadratic on system input $u(t)$ and linear on dummy input $u_d(t)$. The importance of weighting the dummy input is described in [12]. The resulting performance index Eq. (11),

has been scaled in order to reduce numerical errors in the optimization and contains

$$\begin{aligned} \phi &= 0 \\ L &= 2 \times 10^{-4} \sum_{i=1}^{n} f_{qa}\left((x)_i - x_{sp}, 0.001, 0.999\right) \\ &+ 0.02\ u_n^T u_n - 2 \times 10^{-7} \sum_{i=1}^{m_c} u_{d,i}. \end{aligned} \quad (25)$$

C. Controller implementation and simulation setup

The NMPC simulation has been implemented in MATLAB® using C functions (through MEX files) to explicitly calculate Jacobians H_u and H_x. The C functions are generated using AutoGenU: An Automatic Code Generation System for Nonlinear Receding Horizon Control [13]. AutoGenU evaluates the Jacobians using symbolic mathematics in Mathematica® and saves them as C functions that can be used in MATLAB® simulations.

The numerical integrations of ODE's corresponding to state and costate dynamics are performed using explicit Forward Euler method with constant integration step. The method has been chosen because the circuit dynamics is stiff and relatively small time steps of integration are necessary. The maximum length of the time step assuring convergence of the numerical integration Δt_{max} has been estimated based on eigenvalues analysis of linearized system equation $f(x,u)$ as $\Delta t < \Delta t_{max} < c\Delta_{\frac{dT}{dx}}^{\frac{2}{3}} N_x^{-2}$ with N_x spatial discretization points of the PDE describing system dynamics, temperature gradient error introduced by stiffness reduction $\Delta_{\frac{dT}{dx}}$ and parameter c corresponding to circuit properties. The integral of $H_{u,i}$ and C_i is approximated using rectangle quadrature method with one subinterval per integration interval.

In the simulation two thermally coupled Standard Cells of the SHCC are controlled using two BHX input coolant mass flow rates. Two inequality constraints posed on the coolant flows need 2 dummy variables. Thus the dimensions of corresponding input vectors are $m_u = 4$ and $m_c = 2$. A single simplified model used in the controller is discretized using 5 points. Thus, for two cells, dynamics of 10 states and costates have to be integrated over control horizon with maximum time step calculated $\Delta t_{max,o} = 5.54$ s. The setpoint x_{sp} is the same for interconnected cells. The C/GMRES needs an initial optimal trajectory to be provided at the start of simulation. In order to facilitate the calculation of the initial trajectory, the length of the control horizon starts from $T(0) = 0$. Then it is gradually increased to its final value $\lim_{t\to\inf} T(t) = 30$ min, see Fig. 3. The control horizon is subdivided into $N = 10$ equal intervals and input value is kept constant over each interval, as explained at the beginning of the section. The control input is recalculated every 60 seconds of simulated time. In the simulation the controlled circuit has been represented by different, more precise circuit model than that used in the controller. The model includes dynamics of saturation effects in the BHX, uses higher discretization number, 20 points per cell, and allows simulation of heat load perturbations effects. Heat loads are estimated based on energy balance for a double cell and neglecting fluid accumulation in the BHX.

D. Performance of the controller

The important, observed features of the C/GMRES method are its low computing cost and the fact that the residuum of the optimality condition quickly converges back to zero after perturbing the system. The optimization problem contains 60 free variables, $N(m_u + m_c) = 10(4 + 2) = 60$, and has to be solved every 60 seconds of the simulated time. Less than 0.5 s are needed for computing the optimal control trajectory on a personal computer with 2.4 GHz CPU, which is $60/0.5 = 120$ times smaller than time available for calculation. The low computational cost of C/GMRES makes possible further development of the controller: introduction of remaining operational constraints related to BHX overflow and maximal magnets temperature. The next step would be further extension to NMPC of the SHCC over whole LHC sector under constraints imposed by the pumping capacity of common compressor unit and taking into account the pressure drop in the 3.3km long helium distribution line.

In the preliminary study, NMPC action has been simulated in presence of heat load perturbations and errors due to modeling but without BHX pressure perturbations. Comparing the NMPC simulation results, Fig. 3, with that of a PI control in the same conditions, Fig. 2, we observe different closed loop system dynamics. In case of NMPC, offsets between the setpoint and maximal magnet temperature in each cell are observed. Small, positive offset, proportional to heat load, appears in one cell because the cost function f_{qa} is only an approximation of the control objective. Significant, negative offset in the other cell is due the fact that the NMPC tends to equally redistribute the coolant mass flow rate over two cells, thus to reduce heat flows between them due to thermal coupling. In contrast PI controller stabilizes at the setpoint the maximum temperature in each cell separately that causes increased heat flows between cells and vanishing coolant flow in one cell. One problem that has not been addressed relates to finite rangeability of the control valve, which means that mass flow rate cannot be controlled in range $0 < W_{in} < 0.6$ g/s and a cost function should be developed to limit setting input inside of that range.

IV. CONCLUSIONS

The new simplified, first principles, distributed parameter model of Standard Cell of the SHCC has been reviewed. Despite of its simplicity, the model captures the most important features of nonlinear temperature dynamics of the main superconducting magnets. These are related to physical properties of superfluid helium and cooling power distribution of the BHX. An important operational constraint of the circuit, heat exchanger overflow, can be estimated using the model. Moreover, the model can be used for simulation of interconnected Standard Cells, up to the whole sector of the LHC.

The application of the NMPC to stabilization of the maximal superconducting magnets temperature has been

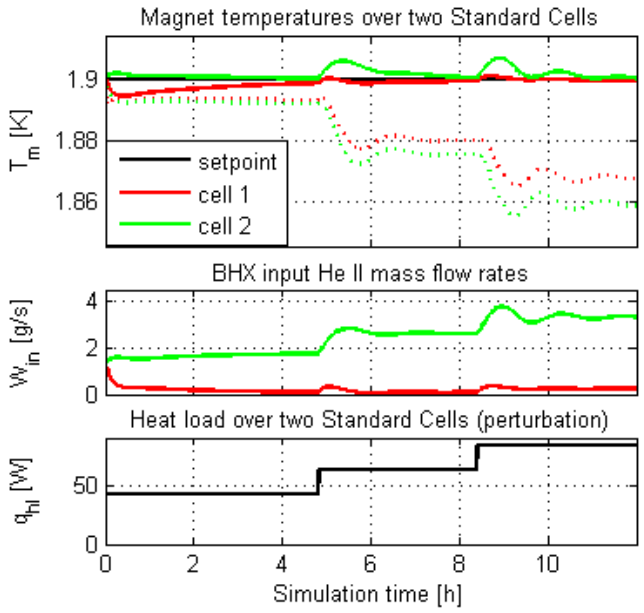

Fig. 2. Simulated performance of PI control applied to the SHCC. In upper plot, four magnet temperatures correspond to maximal (solid line) and minimal (dotted line) value in each of two interconnected Standard Cells.

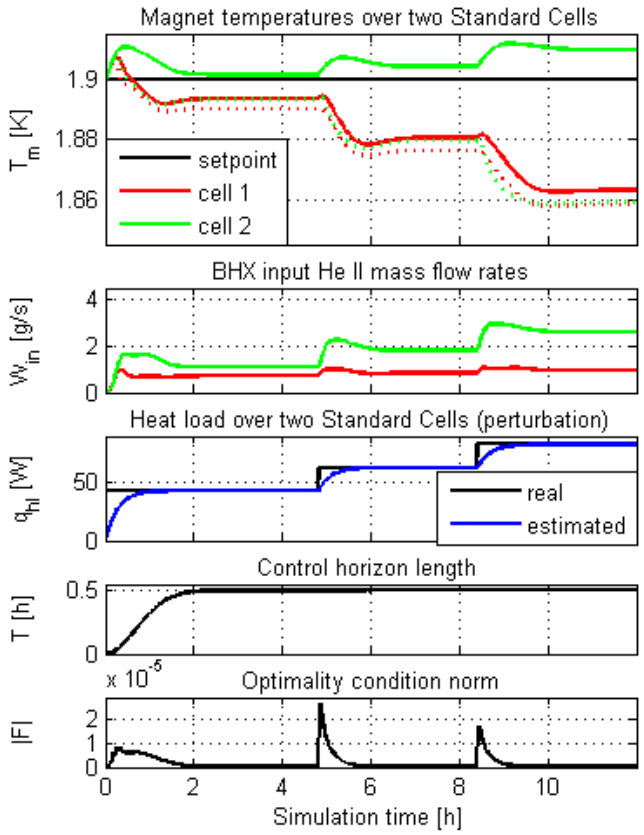

Fig. 3. Simulated performance of NMPC control applied to the SHCC. In upper plot, four magnet temperatures correspond to maximal (solid line) and minimal (dotted line) value in each of two interconnected Standard Cells.

studied based on the simplified model. The simulation of NMPC using C/GMRES algorithm has been implemented using MATLAB® and C code. The C functions calculating analytical Jacobians H_u and H_x are generated using AutoGenU. Preliminary simulation results are promising. The very low computational cost of the NMPC online optimization using C/GMRES solution/approximation method has been observed, proving the real-time feasibility of the NMPC application. However, the quadratic asymmetric cost function used to approximate the control objective introduces offset between setpoint and the maximal temperature and should be improved.

V. ACKNOWLEDGMENTS

The authors would like to thank for the support provided by project DPI2006-13593, CERN, University of Valladolid, Osaka University and Japan Student Services Organization. Members of CERN, University of Valladolid, Ohtsuka Lab and the control engineering community have contributed to this work with helpful comments and suggestions.

REFERENCES

[1] CERN Press Office, "LHC research programme gets underway," CERN Press Release, 2010. [Online]. Available: http://public.web.cern.ch/press/pressreleases/Releases2010/PR07.10E.html

[2] O. S. Brüning, P. Collier, P. Lebrun, S. Myers, R. Ostojic, J. Poole, and P. Proudlock, *LHC Design Report*. Geneva: CERN, 2004. [Online]. Available: http://cdsweb.cern.ch/record/782076

[3] P. Lebrun, L. Serio, L. Tavian, and R. Van Weelderen, "Cooling Strings of Superconducting Devices below 2 K: the Helium II Bayonet Heat Exchanger," *Adv. Cryog. Eng., A*, vol. 43, pp. 419–426, Sep 1997. [Online]. Available: http://cdsweb.cern.ch/record/336315/

[4] B. Flaemster, "Investigation, Modelling and Control of the 1.9 K Cooling Loop for Superconducting Magnets for the Large Hadron Collider," Ph.D. dissertation, Trondheim TU, Geneva, 2000. [Online]. Available: http://cdsweb.cern.ch/record/433397/

[5] E. Blanco, "Nonlinear Model-based Predictive Control Applied To Large Scale Cryogenics Facilities," Ph.D. dissertation, University of Valladolid, 2001.

[6] E. Blanco, C. de Prada, S. Cristea, and J. Casas, "Nonlinear predictive control in the LHC accelerator," *Control Eng. Pract.*, vol. 17, no. 10, pp. 1136 – 1147, 2009. [Online]. Available: http://dx.doi.org/10.1016/j.conengprac.2009.04.007

[7] P. Gomes, C. Balle, E. Blanco-Viñuela, J. Casas-Cubillos, S. Pelletier, M. A. Rodrguez, L. Serio, A. Suraci, and N. Vauthier, "Experience with the String2 Cryogenic Instrumentation and Control System," no. CERN-LHC-Project-Report-794, Sep 2004. [Online]. Available: http://cdsweb.cern.ch/record/795003/

[8] R. Srinivasan and A. Hofmann, "Investigations on cooling with forced flow of He II. Part 2," *Cryogenics*, vol. 25, no. 11, pp. 652 – 657, 1985. [Online]. Available: http://dx.doi.org/10.1016/0011-2275(85)90121-3

[9] D. Camacho, S. Chevassus, C. Policella, J. M. Rieubland, G. Vandoni, and R. Van Weelderen, "Thermal Characterization of the HeII LHC Heat Exchanger Tube," no. CERN-LHC-Project-Report-232, Aug 1998. [Online]. Available: http://cdsweb.cern.ch/record/365293/

[10] A. E. Bryson and Y.-C. Ho, *Applied optimal control : optimization, estimation, and control*. Hemisphere Pub. Corp., 1975.

[11] T. Ohtsuka, "A continuation/GMRES method for fast computation of nonlinear receding horizon control," *Automatica*, vol. 40, no. 4, pp. 563 – 574, 2004. [Online]. Available: http://dx.doi.org/10.1016/j.automatica.2003.11.005

[12] H. Seguchi and T. Ohtsuka, "Nonlinear receding horizon control of an underactuated hovercraft," *Internat. J. Robust Nonlinear Control*, vol. 13, no. 3 - 4, pp. 381–398, 2003. [Online]. Available: http://dx.doi.org/10.1002/rnc.824

[13] T. Ohtsuka, "AutoGenU: Readme.txt," 2000. [Online]. Available: http://www-sc.sys.es.osaka-u.ac.jp/~ohtsuka/code/